Published in final edited form as:
Sci Transl Med. 2014 March 26; 6(229): 229ra43. doi:10.1126/scitranslmed.3007965.

Cytotoxicity of paclitaxel in breast cancer is due to chromosome missegregation on multipolar spindles

Lauren M. Zasadil[1,2], **Kristen A. Andersen**[2], **Dabin Yeum**[1], **Gabrielle B. Rocque**[3], **Lee G. Wilke**[4,5], **Amye J. Tevaarwerk**[3,5], **Ronald T. Raines**[5,6], **Mark E. Burkard**[3,5], and **Beth A. Weaver**[1,5,*]

[1]Department of Cell and Regenerative Biology, University of Wisconsin, Madison, WI 53705, USA

[2]Cellular and Molecular Pharmacology Training Program, University of Wisconsin, Madison, WI 53705, USA

[3]Department of Medicine, University of Wisconsin, Madison, WI 53705, USA

[4]Department of Surgery, University of Wisconsin, Madison, WI 53705, USA

[5]Carbone Cancer Center, University of Wisconsin, Madison, WI 53705, USA

[6]Departments of Biochemistry and Chemistry, University of Wisconsin, Madison, WI 53705, USA

Abstract

The blockbuster chemotherapy drug paclitaxel is widely presumed to cause cell death in tumors as a consequence of mitotic arrest, as it does at concentrations routinely used in cell culture. However, we determine here that paclitaxel levels in primary breast tumors are well below those required to elicit sustained mitotic arrest. Instead, cells in these lower concentrations of drug proceed through mitosis without substantial delay and divide their chromosomes on multipolar spindles, resulting in chromosome missegregation and cell death. Consistent with these cell culture data, the majority of mitotic cells in primary human breast cancers contain multipolar spindles after paclitaxel treatment. Contrary to the previous hypothesis, we find that mitotic arrest is dispensable for tumor regression in patients. These results demonstrate that mitotic arrest is not responsible for the efficacy of paclitaxel, which occurs due to chromosome missegregation on highly abnormal, multipolar spindles. This mechanistic insight may be used to improve selection of future anti-mitotic drugs and to identify a biomarker with which to select patients likely to benefit from paclitaxel.

Introduction

Paclitaxel is the best selling chemotherapy drug in history, and is currently used to treat patients with a variety of cancers, including those of the breast, lung, and ovaries (1, 2).

*To whom correspondence should be addressed: Beth A. Weaver, University of Wisconsin - Madison, 1111 Highland Avenue, 6109 WIMR, Madison WI 53705-2275, Tel: (608) 263-5309, Fax: (608) 265-6905, baweaver@wisc.edu.

Author Contributions: The manuscript was written by LMZ, MEB, and BAW. KAA, DY, GBR, LGW, AJT, and RTR edited the manuscript. Experiments were performed by LMZ and KAA. DY assisted with experiments. Patient biopsies were obtained by GBR, LGW, AJT, and MEB. Experiments were designed by RTR, MEB, and BAW.

Competing interests: The authors declare that they have no competing interests.

Paclitaxel is a microtubule poison (3) that arrests cells in mitosis (4, 5) due to activation of the mitotic checkpoint (also known as the spindle assembly checkpoint), the major cell cycle checkpoint that regulates progress through mitosis (6–8). Unlike previously identified microtubule toxins, which result in microtubule depolymerization, paclitaxel promotes microtubule assembly and stabilization (3, 5, 9). Lower concentrations of paclitaxel suppress the rate at which microtubules grow and shrink, without substantially increasing microtubule polymer mass, while still arresting cells in mitosis on bipolar spindles (4, 10, 11).

Cells arrested in mitosis can either die during that mitosis or undergo a process known as mitotic slippage, in which they enter G1 without undergoing anaphase or cytokinesis to produce a single, tetraploid cell. Cells may arrest, cycle, or die after slippage (12–14). What determines the outcome of mitotic arrest currently remains unknown. In an elegant series of experiments, chromosomally stable, non-transformed cells were followed by timelapse microscopy to identify daughter cells that originated from the same parent through a division that did not include chromosome missegregation. Even these genetically identical daughters exhibited differing responses to mitotic arrest (15).

Although serum concentrations of paclitaxel have been measured (16–18), paclitaxel is known to accumulate intracellularly at levels up to and exceeding 1000-fold, depending on cell type and concentration (4, 11, 19). Thus, the clinically relevant, intratumoral concentration of paclitaxel in breast cancer has never been determined.

In this study, we measured the intratumoral paclitaxel concentration in naïve breast tumors from patients receiving neoadjuvant paclitaxel and correlated it with treatments used in cell culture to establish a clinically relevant concentration range. At clinically relevant paclitaxel concentrations, cells did not show a substantial mitotic arrest. Instead, they completed mitosis on multipolar spindles, resulting in chromosome missegregation. Patient tumors treated with paclitaxel exhibited multipolar spindles, and mitotic arrest was not required for tumor regression. These results demonstrate that paclitaxel-mediated cell death in patient tumors is due to chromosome missegregation on abnormal mitotic spindles.

Results

Paclitaxel has concentration-dependent effects in cell culture

Because the concentration of paclitaxel that mimics the intratumoral concentration was unknown, we initially sought to determine whether paclitaxel exerted similar effects over a broad concentration range in breast cancer cells in culture. The triple negative breast cancer cell lines MDA-MB-231 and Cal51, which are negative for the estrogen receptor, the progesterone receptor and human epithelial growth factor receptor 2 (HER2), were treated with paclitaxel concentrations spanning five orders of magnitude. Bipolar spindles have previously been reported after paclitaxel treatment (4, 10, 20). However, we observed multipolar spindles in all concentrations of paclitaxel tested (Fig. 1A), the incidence of which rose with increasing drug concentration (Fig. 1B and C).

Distinct concentrations of paclitaxel also differed in their ability to induce mitotic arrest. After micromolar (μM) paclitaxel treatment, both MDA-MB-231 and Cal51 cells displayed

a substantial increase in mitotic index, indicative of mitotic arrest, as expected (Fig. 1D and E). In even higher concentrations of paclitaxel, the mitotic index was reduced, as has been previously reported to occur due to the ability of the large mass of polymerized tubulin to satisfy the mitotic checkpoint through syntelic chromosome attachments (21, 22). More subtle effects on mitotic index were observed in low nanomolar (nM) concentrations of paclitaxel (Fig. 1D and E).

Timelapse videomicroscopy was used to determine the influence of paclitaxel on duration of mitosis (measured as the time from cell rounding to the flattening of the first daughter cell). Similar to mitotic index, the duration of mitosis rose, peaked, and then declined in response to increasing concentrations of paclitaxel (Fig. 1F and G). Thus, paclitaxel exhibits concentration-dependent effects in cell culture, emphasizing the need to identify the clinically relevant dose(s) to study in cell culture and animal models.

Mitotic arrest is not required for response to paclitaxel

To determine the clinically relevant concentration of paclitaxel, we designed a clinical trial to enroll six female patients with newly diagnosed, locally advanced breast cancer, who had not received prior treatment. One patient was excluded from analysis due to insufficient tumor tissue in the post-paclitaxel biopsy. Enrolled patients ranged in age from 42 to 65 and had Nottingham grade 2 or 3 tumors (Table 1). To minimize confounding variables, patients with HER2-amplified tumors were not enrolled, since these patients receive HER2 targeted antibody therapy in combination with chemotherapy.

The research protocol is depicted in Figure 2A. After diagnostic core needle biopsy, initial tumor measurements were obtained using mammography, ultrasound, or both. Patients were then treated with 175 mg/m^2 neoadjuvant paclitaxel infused over 3 hours. A second tumor biopsy was obtained 20 hours after initiation of the paclitaxel infusion and was divided into two parts. One part was flash frozen to measure paclitaxel levels, while the other was fixed for histological analysis. Blood was also collected at this time point to measure the concentration of paclitaxel in serum. The 20 hour time point was selected because breast cancer cells in culture mounted a robust mitotic arrest after 20 hours of treatment (Fig 1). Mitotic index was elevated ≥15 fold from 16 hours through at least 32 hours after paclitaxel administration in both cell lines (Fig S1). Therefore, we predict that an increase in mitotic index as a consequence of paclitaxel would be apparent at 20 hours.

After the initial infusion of paclitaxel and the second biopsy, patients completed an additional 3 standard cycles of paclitaxel administered every two weeks. Tumors were again evaluated by mammography, ultrasound, or both, approximately two weeks after the final dose of paclitaxel. Finally, patients received 4 cycles of the DNA damaging drugs Adriamycin/doxorubicin and cyclophosphamide (AC) prior to surgery.

To determine whether patients responded to paclitaxel treatment, tumor measurements were obtained at baseline and after the completion of paclitaxel therapy (prior to initiation of AC) by mammogram (Fig. 2B) and/or ultrasound (Fig. 2C–D). Tumor response was evaluated according to Response Evaluation Criteria in Solid Tumors (RECIST) 1.1 guidelines (23).

Partial tumor response, determined as ≥30% decrease in the largest tumor diameter, was observed in patients 1–3, but not 4–6 (Fig. 2E).

To determine whether patient response correlated with mitotic arrest, tumor sections prior and subsequent to paclitaxel therapy were analyzed by immunofluorescence. Phosphorylated histone H3 (pH3) and DAPI were used to identify mitotic cells. Tumor sections were co-stained for cytokeratin to distinguish breast tumor epithelial cells from stroma (Fig. 2F and G). Mitotic cells were detected in all tumor samples. Tumors from patients 4 and 6 exhibited an increase in mitotic index in response to paclitaxel treatment (Fig. 2F), consistent with mitotic arrest, although these tumors only minimally regressed in response to paclitaxel (Fig. 2D and E). In contrast, the tumor from patient 3 shrank markedly in response to paclitaxel (Fig. 2B, C and E), despite a decline in mitotic index (Fig. 2F). Thus, mitotic arrest is not a prerequisite for efficacy of paclitaxel.

Clinically relevant doses of paclitaxel are in the low nM range

Paclitaxel is known to accumulate intracellularly at levels that vary from 67- to over 1000-fold, depending on cell type and concentration (4, 11, 19). To determine the amount of intratumoral accumulation in breast cancer patients, paclitaxel concentrations were measured by HPLC analysis in patient plasma and tumor samples obtained 20 hours after initiation of the first paclitaxel infusion (Table 2). Patient plasma concentrations of paclitaxel ranged from 80–280 nM, in good agreement with previous measurements (16–18). Paclitaxel concentrations in patient tumors were measured both by volume and by weight, which were in good agreement (Table 2, Table S1). Intratumoral concentrations ranged from 1.1 to 9.0 μM as calculated using tumor weight, representing a degree of concentration of 4- to 70-fold (Table 2).

To identify the concentration(s) of paclitaxel with which to treat MDA-MB-231 and Cal51 cells to mimic the clinically relevant intratumoral concentration, a range of paclitaxel concentrations was added to the media of MDA-MB-231 and Cal51 breast cancer cells. Cells were collected 20 hours later. Intracellular paclitaxel concentration was measured using HPLC. The uptake of paclitaxel ranged from 8- to 1600-fold (Table 3). In both cell lines, lower amounts of added paclitaxel resulted in higher degrees of concentration (Table 3), as has been observed previously (4, 11, 19). Also consistent with previous reports, the different cell lines varied in their level of paclitaxel uptake, resulting in distinct intracellular concentrations [Table 3; (19)]. Addition of low concentrations of paclitaxel, which were not sufficient to cause substantial mitotic arrest (Fig. 1D through G), resulted in intracellular concentrations analogous to those in patient tumors in both MDA-MB-231 and Cal51 cells (Table 3).

Low concentrations of paclitaxel are sufficient to cause cell death

Paclitaxel-mediated cell death is generally studied at concentrations that cause mitotic arrest, in part because higher levels of drug produce death more rapidly (11, 24). To test whether low concentrations of paclitaxel are sufficient to cause cell death, ≤100 nM paclitaxel was added to MDA-MB-231 and Cal51 cells, which were incubated for an additional 24, 72, or 120 hours. Indeed, clinically relevant paclitaxel concentrations were sufficient to cause a

substantial reduction in live cells (Fig. 3A) and an increase in dead cells (Fig. 3B). These effects were particularly apparent over the longest time course of 120 hours. To assess the impact of clinically relevant concentrations of paclitaxel on colony-forming ability, cells were plated at low density and grown in the presence or absence of paclitaxel for 14 days. Colony formation was substantially inhibited by paclitaxel concentrations ≥5 nM in both MDA-MB-231 and Cal51 cells (Fig. 3C). Thus, clinically relevant concentrations of paclitaxel induce cell death and inhibit proliferation in cell culture.

Clinically relevant concentrations of paclitaxel cause chromosome missegregation

The analysis of fixed cells in Figure 1A through C suggested that cells entering mitosis in intratumoral concentrations of paclitaxel would develop multipolar spindles which, upon DNA segregation, are predicted to give rise to aneuploid progeny. To test this hypothesis, chromosome number per cell was analyzed by counting chromosomes in metaphase/chromosome spreads. Cal51 cells were used for this analysis because they are a near-diploid, chromosomally stable cell line, whereas MDA-MB-231 cells are chromosomally unstable. 48 hours of treatment with 5, 10, or 50 nM paclitaxel substantially increased the incidence of near-diploid aneuploidy, with little evidence of tetraploidy, in the mitotic populations analyzed (Fig. 4A through C).

These data suggested that, in clinically relevant concentrations of drug, cells proceed through mitosis after only a brief delay on multipolar spindles to produce aneuploid progeny. To test this directly, cell lines expressing GFP-tubulin and RFP-histone H2B were observed using timelapse microscopy in the presence or absence of low nM paclitaxel (Fig. 4D, S2A, and Supplementary Videos 1–6). Indeed, while cells often initially assembled a bipolar mitotic spindle in the presence of low concentrations of paclitaxel, additional spindle poles frequently developed before anaphase onset (Fig. 4D, S2A, Supplementary Videos 5–6). In some cases, multipolar spindles coalesced before anaphase onset into bipolar spindles, as reflected by the difference between incidences of multipolar spindle formation and > 2-way DNA divisions (Fig. 4E and S2B). However, many cells divided their chromosomes in three or more directions once they entered anaphase (Fig. 4D and E, S2A and B, Supplementary Videos 2, 3, 5 and 6). The number of directions in which the chromosomes were separated was not necessarily predictive of the number of cells generated, as DNA segregated to two or more spindle poles could be incorporated into the same daughter cell (Fig. 4D, S2A, Supplementary Videos 2, 3, 5 and 6).

In Cal51 cells, 10 and 50 nM paclitaxel increased the percentage of abnormal mitoses from 5.5% to 34.5% and 54.5% respectively, predominantly due to multipolar spindles and divisions, rather than lagging chromosomes (Fig. 4E and Supplementary Videos 1–3). In the portion of Cal51 cells in which nuclear envelope breakdown (NEB) was observed, 4 of the 14 cells that initially established a bipolar spindle developed additional spindle poles before anaphase onset. Only 2 of the 7 cells which formed multipolar spindles upon NEB focused them to become bipolar.

MDA-MB-231 cells, like a large percentage of human breast cancers, exhibit chromosomal instability. Even for this cell line, in which 53% of unperturbed cells underwent an abnormal division, primarily due to lagging chromosomes during anaphase or the failure to align all

chromosomes at the metaphase plate [Fig. S2B; (25)], addition of 5 or 10 nM paclitaxel increased the percentage of mitoses exhibiting at least one mitotic abnormality to 100% (Fig. S2B and Supplemental Videos 4–6).

To test whether spindle multipolarization occurs as a generic consequence of mitotic delay, Cal51 cells were arrested in mitosis with the proteasome inhibitor MG132. 0 of 16 cells developed multipolar spindles during an arrest of ≥3 hours. Twelve of these cells were arrested for ≥10 hours without the formation of additional poles, demonstrating that the additional spindle poles seen in paclitaxel treated cells are not simply a result of delayed mitosis.

Clinically relevant concentrations of paclitaxel cause death in interphase only after a perturbed mitosis

Our data suggest that clinically relevant concentrations of paclitaxel result in cell death after chromosome missegregation. High rates of chromosome missegregation have previously been shown to result in rapid cell death in tumor cells, independent of p53 status (26–28). However, a proposed alternate hypothesis is that paclitaxel kills cells in interphase, without passing through mitosis, due to altered microtubule transport (29). Microtubules have known functions in maintaining proper Golgi structure and a functional secretory pathway. We therefore tested whether this could explain our findings. Depolymerization of microtubules with vinblastine resulted in dispersion of the Golgi [(30); Fig. S3A–B]. However, Golgi structure appeared unaffected by clinically relevant concentrations of paclitaxel, and higher concentrations had only a subtle effect compared with vinblastine (Fig. S3C–D).

To directly test whether paclitaxel-mediated cell death occurred in interphase, cells were observed by timelapse microscopy to determine in which stage of the cell cycle death occurred. In clinically relevant concentrations of paclitaxel, the majority of cell death was seen during or after mitosis in both MDA-MB-231 and Cal51 cells (Fig. S4A and B). In higher concentrations of drug, cell death was also predominantly seen during or after mitosis, although there was a minor increase in cell death in interphase cells that had not passed through mitosis in the presence of paclitaxel (Fig. S4A and B).

To test whether paclitaxel could induce cell death in interphase cells prior to division, cells were arrested in S phase for 72 hours with thymidine in the presence or absence of paclitaxel (Fig. S4C). The addition of any concentration of paclitaxel did not cause substantial decreases in the live cell population of MDA-MB-231 cells (Fig. S4D). Only micromolar concentrations of paclitaxel caused substantial cell death from interphase in Cal51 cells (Fig. S4E).

Levels of proliferation in patient tumors, as scored by Ki67 reactivity, were substantial enough to be congruent with an anti-mitotic effect of paclitaxel, and were unchanged by 20 hours of paclitaxel therapy (Fig. S5), suggesting that paclitaxel did not cause widespread quiescence in interphase cells. This evidence suggests that, at clinically relevant concentrations, death from interphase occurs only when a preceding mitosis is perturbed by paclitaxel.

Paclitaxel induces multipolar spindles in patient tumors

To verify that effects observed on mitosis in cell culture also occurred in patient tumors, tumor sections were analyzed by immunofluorescence to determine spindle pole number (Fig. 5A). Spindle poles were labeled with Nuclear Matrix Apparatus protein (NuMA), and centrosomes were identified with γ-tubulin. A majority of mitotic cells in patient tumors exhibited >2 NuMA-labeled spindle poles (Fig. 5A–B). This occurred even in cells with only two γ-tubulin labeled centrosomes (Fig. 5A, top and center rows), and additional spindle poles did not co-localize with γ-tubulin, demonstrating that centrosome amplification and/or splitting is not necessary for paclitaxel to induce multipolar spindles in patients. Misaligned chromosomes were also observed in cells containing bipolar spindles (Fig. 5A, asterisks in bottom row), suggesting that initially multipolar spindles had later clustered their spindle poles to become bipolar, as has been reported previously in cell culture (31).

A portion of patient samples exhibited multipolar spindles prior to paclitaxel treatment, as has been previously reported in cancers and malignant cell lines (32, 33). However, paclitaxel resulted in an increase in the incidence of multipolar spindles in all patient samples observed (Fig. 5B), consistent with our findings in cell culture (Fig. 1B and C, 4D and E, S2A and B). Interestingly, the highest percentages of multipolar spindles were reached in patients 1 and 3, who also had the largest level of tumor regression (Fig. 2E and 5B).

Discussion

Paclitaxel entered human trials in 1984, and has since become a widely used chemotherapeutic agent. Extensive studies have been performed to delineate its effects on purified tubulin and cultured cells, as well as its efficacy in a wide range of tumors. Although it is considered a highly effective agent in breast cancer, a substantial proportion of treated patients are primarily resistant to paclitaxel therapy. Biomarkers predicting which patients will respond to paclitaxel would be indispensable, yet remain elusive. In part, this may be because most studies have focused on concentrations of paclitaxel that cause mitotic arrest and rapid cell death, but are unlikely to be achieved in patient tumors. Here we demonstrate that, contrary to the predominant hypothesis that paclitaxel causes cell death as a consequence of mitotic arrest, intratumoral concentrations result in chromosome segregation on multipolar spindles, producing aneuploid progeny. Cell death occurs with slower kinetics than when higher concentrations of drug are used, and presumably occurs due to loss of both copies of one or more essential chromosomes. This is likely to account for the time delay between the formation of abnormal mitotic spindles and the onset of substantial cell death in a population, suggesting that sufficient time must be spent in the presence of paclitaxel for a large proportion of the cell population to have undergone aberrant, lethal mitoses, which may not occur during the first division in the presence of drug. Consistent with this, the percentage of cell death increases with time spent in paclitaxel. Although passage through mitosis on multipolar spindles can and does result in cell death, a portion of cells may also arrest or slow their cell cycle progression after a multipolar division, as suggested by stronger effects on live cell number and colony forming

ability than on cell death in Cal51 cells treated with 5 nM paclitaxel. These mechanistic insights may enable the development of a biomarker to predict paclitaxel response.

Previous reports of intratumoral paclitaxel concentrations in humans are exceedingly limited given the large body of paclitaxel literature. Measurements that have been reported are in μg per gram of tumor tissue, and the density of the tumor is required to convert these measurements into concentrations used in cell culture (μM or μg/mL). Prior to this study, we were uncertain whether the density of tumors differed significantly from that of water. Encouraged by the agreement in our measurements of paclitaxel concentration by weight and by volume, we converted previous studies' measured levels of paclitaxel in tumors to molar concentrations. Paclitaxel concentrations measured in brain tumors 2–3 hours after a 3 hour administration of 175 mg/m^2 drug were approximately 3 μM (34), which is in the range of 1 to 9 μM we measured 20 hours after administration of the same dose to breast cancer patients. Uterine cervical cancer patients treated with 60 mg/m^2 paclitaxel per week for 2–4 weeks had approximately 400 nM paclitaxel remaining in their tumors 6 days after the final dose was administered (35). These results suggest that paclitaxel levels are not appreciably higher at earlier timepoints than at 20 hours, and indicate that paclitaxel is retained in tumor tissue (at least in uterine cervical tumors) for a substantial period of time.

Prior to this work, the major alternative to the hypothesis that paclitaxel causes anticancer effects as a consequence of mitotic arrest was that it causes cell death in interphase without affecting mitosis (29, 36). A key argument for the alternate hypothesis of interphase action is that human tumors have a slow doubling time, suggesting that an insufficient proportion of cells pass through mitosis in the presence of paclitaxel for mitosis to be its target. However, tumor doubling time is a measure of both proliferation and cell death, which is prevalent in untreated tumors. Indeed, tumor doubling times have been estimated to be <5 percent of what would be predicted based on proliferative rates (37–40). Patient samples obtained in this study displayed rates of proliferation sufficient for the anti-mitotic effects of paclitaxel to account for its cytotoxicity. The mitotic index (the percentage of mitotic epithelial cells) in patient tumors prior to paclitaxel administration was 0.4, 1.3, 2.2, 2.3, and 3.9%. This is in the range of primary murine embryonic fibroblasts, which have a mitotic index of 2.0–2.5%, and are commonly used for mitotic analysis (41–44). The extended retention of paclitaxel in uterine cervical cancers (35), coupled with the failure of paclitaxel to reduce the proliferative index of breast tumors, strongly suggests that a sufficient number of dividing cells pass through mitosis in the presence of paclitaxel to allow for substantial cytotoxic effects in sensitive tumors.

A second argument for paclitaxel enacting cell death from interphase is that paclitaxel-induced mitotic arrest does not necessarily lead to response to paclitaxel in syngeneic murine (45) or human cancers (46). However, patients with tumors containing a higher mitotic index prior to chemotherapy are more likely to respond to paclitaxel than patients with a lower mitotic index (47). Our results offer the unifying explanation that paclitaxel produces cell death in patients by inducing chromosome missegregation without mitotic arrest.

The success of paclitaxel and other microtubule poisons is limited by peripheral neuropathy, which presumably occurs due to deficits in axonal transport on the longest axons in the body. Because the activity of paclitaxel was attributed to its ability to induce mitotic arrest, this limitation led to the development of novel anti-mitotic drugs that arrest cells in mitosis without disrupting microtubules (48). Anti-mitotic drugs directed against a variety of targets, including Eg5/KSP and the kinases polo and Aurora A, have entered clinical trials (NCT01034553, NCT01510405, NCT01065025). Some have concluded that these drugs lack efficacy (36), although others have argued that this conclusion is premature (49, 50). Our data suggest that inducing mitotic arrest is unlikely to mimic the full range of effects of paclitaxel on mitosis. Although some portion of cell death and tumor regression in response to paclitaxel treatment may arise as a consequence of mitotic arrest, this is clearly not the only mechanism by which paclitaxel exerts its effects. However, these newer anti-mitotic agents may still be able to mimic the chromosome missegregation caused by paclitaxel if dosed continuously at low levels. This effect occurs, for example, from partial loss of polo-like kinase 1 activity (51).

In higher concentrations of paclitaxel, cells frequently slip out of mitosis into G1 without segregating their chromosomes or completing cytokinesis to produce a tetraploid cell with two centrosomes. After centriole duplication in S phase, this can result in the formation of multipolar spindles. However, patient tumors treated with paclitaxel show multipolar spindles without supernumery centrosomes. Additionally, only 2 of 7 Cal51 cells that initially established multipolar spindles were able to focus these to become bipolar. Together, these data suggest that multipolar spindles in clinically relevant doses of paclitaxel occur as a consequence of a failure to efficiently cluster de novo spindle poles rather than because of mitotic slippage.

Recently, two groups used state-of-the-art, high resolution intravital imaging to observe mitosis in xenograft or isograft tumors (52, 53). This is a powerful technique that permits visualization of cell division and death before, during, and after treatment with chemotherapy. By using a photoconvertible fluorophore, the same cells can be marked and imaged over multiple days (53). Hopefully, this powerful technique can now be applied to mammary tumors containing clinically relevant concentrations of paclitaxel.

This study is limited by the small number of patients and the acquisition of biopsies at a single time point after paclitaxel administration. Future studies of paclitaxel concentrations in breast cancer will ideally include a time course of biopsies to determine the kinetics of drug retention in breast tumor tissue. Larger sample sizes will permit a more robust test of the prevalence of multipolar spindles/divisions and whether this correlates with patient response to paclitaxel.

Understanding the mechanism of taxane therapy is crucial to make rational improvements in cancer treatments targeting mitosis. Many efforts have focused on new drugs that elicit mitotic arrest and slippage (54). Our data suggest, instead, that new anti-mitotics might optimally be designed to dysregulate mitosis without eliciting prolonged arrest. Moreover, our study indicates that taxane resistance is primarily related to an enhanced ability to withstand irregular chromosome segregations. Thus, identifying tumors that are more or less

susceptible to missegregation is the key to selection of patients who will and will not benefit from paclitaxel.

Materials and Methods

Study Design

This was a 6-subject non-randomized study of paclitaxel effect on human breast cancer and on breast cancer cell lines MDA-MB-231 and Cal51. The patient sample size was selected to provide a sufficient number of replicates for sampling intratumoral drug concentrations. All subjects had newly diagnosed breast cancer for which neoadjuvant chemotherapy was recommended per standard of care. Subjects received initial chemotherapy with paclitaxel 175 mg/m^2 dosed every two weeks with filgrastim support. Biopsy was obtained 18–22 hours after start of the first infusion. After four cycles of paclitaxel, follow-up imaging or exam was performed to assess response to therapy and patients continued with standard anthracycline-based chemotherapy prior to surgery. One patient was excluded from tissue analysis because of insufficient sample collected by biopsy. The objectives were to measure intratumoral paclitaxel concentrations and effects on mitosis and cell proliferation and compare with response to treatment.

Patients

Patients who volunteered were enrolled in a clinical trial specifying the treatment, biopsy, and analysis plan. The protocol was approved by UW Health Sciences Institutional Review Board, ID 2010-0357, assigned UWCCC protocol number OS10103, conducted in accordance with the ethical standards established in the 1964 Declaration of Helsinki and registered on clinicaltrials.gov (NCT01263613). All subjects provided written informed consent prior to enrollment. Patients were enrolled if they had previously untreated locally advanced breast cancer for which neoadjuvant chemotherapy was indicated. All subjects received four cycles of standard-dose paclitaxel 175 mg/m^2 infused over three hours with biopsy and treatment as outlined in Figure 2A. Biopsies and serum collection were scheduled for 20 hours after initiation of paclitaxel infusion. Actual times between initiation of paclitaxel infusion and tumor biopsies in hours:minutes were 21:06, 19:14, 19:54, 19:39, 18:41 and 19:42 for patients 1 through 6, respectively. There were no major complications from protocol therapy.

Cell culture

MDA-MB-231 and Cal51 breast cancer cells were grown in DMEM supplemented with 10% (vol/vol) FBS, 2 mM L-glutamine, and 50 μg/mL penicillin/streptomycin at 37°C and 5% (Cal51) or 10% (MDA-MB-231) CO_2. RFP-tagged histone H2B and GFP-tagged α-tubulin were stably integrated into MDA-MB-231 cells by transfection in a pBabe vector, and into Cal51 cells by lentiviral infection (Millipore LentiBrite™). Single clones were isolated with cloning cylinders (MDA-MB-231) or by single-cell sorting (Cal51). All paclitaxel and MG132 used in cell culture were dissolved in DMSO. Final concentration of DMSO in media was 0.1%. Chromosome spreads and immunofluorescence were performed as in (25). Staining was performed with antibodies to α-tubulin (YL½; Serotec) and Golgin-97 (Life Technologies).

Thymidine block

1×10^5 cells/well were seeded in 12-well plates. After 24 hours, thymidine (2.5 mM for MDA-MB-231, 5 mM for Cal51) +/− indicated concentrations of paclitaxel was added. 72 hours after drug treatment, cells were collected and scored by trypan blue exclusion.

High-Performance Liquid Chromatography (HPLC)

Cells in 10-cm and 15-cm (5 nM paclitaxel condition only) dishes were treated with the indicated concentrations of paclitaxel in 20 mL total volume (50 mL for 15 cm). After 20 hours, cells were pelleted, resuspended in 1 mL ddH_2O, and stored at −80°C. Thawed cells were sonicated in water, and patient biopsies were homogenized in water prior to application to the column. Cell, tumor biopsy, or patient plasma samples were applied to C18 Bond Elut solid-phase extraction columns (Agilent). Paclitaxel was eluted from the Bond Elut columns with acetonitrile. Solvent was removed with a speedvac and samples were reconstituted in 100 μL of HPLC mobile phase. Analysis was performed by monitoring the signal of a 50 μL injection at 227 nm during an isocratic elution with 60% 35 mM acetic acid, 40% acetonitrile on an analytical HPLC instrument (Waters system equipped with Waters 996 photodiode array detector, Empower 2 software, and a Waters Nova-Pak C18 4-μm 4.6 × 150 mm column).

Immunohistochemistry

Five-micrometer sections of formalin-fixed, paraffin-embedded tissue sections were subjected to antigen retrieval in citrate buffer, serum-blocked, and stained with rabbit anti-NuMA antibody [a kind gift from Duane Compton; (55)], γ-tubulin (Sigma), Ki67 (Dako), cytokeratin (to mark epithelial cells; Abcam), and/or pH3 (Cell Signaling) antibodies overnight at 4°C. Alexa Fluor-conjugated secondary antibodies (Invitrogen) were used. DNA was stained using DAPI.

Microscopy

Images were acquired on a Nikon Ti-E inverted microscope with focus-drift compensation using a CoolSNAPHQ2 camera driven by Nikon Elements software. Images are single *z*-planes acquired using a 100×/1.4 numerical aperture (NA) (Fig. 4A) or a 20×/0.1 NA objective (Fig. 2G and S5A). Multipolar spindle examples were acquired using HDR imaging and a 100×/1.4 NA objective. Images in Fig. 5A and S3 are maximum projections from 0.2 μm *z*-stacks collected with a 100×/1.4 NA objective after deconvolution using the AQI 3D Deconvolution module in Elements. Overlays were generated in Photoshop.

For phase-contrast timelapse analysis, cells were placed under 10% CO_2 flow at ~30 mL/min in a heated chamber at 37°C. Images were acquired at 10-min intervals using a 10×, 0.13 NA objective. For fluorescence timelapse analysis, five (MDA-MB-231) or seven (Cal51) 2 μm z-planes were acquired every 2 min using a 60×/1.4 NA objective. Maximum projections of in-focus planes (MDA-MB-231) or the maximally focused single z plane (Cal51) were assembled in Elements, exported as jpg files, and converted to .mov files in QuickTime. Cal51 cells were treated with paclitaxel for 20 hours before observation.

Statistical Analysis

Statistical analysis was performed using Mstat 5.5 software (http://www.mcardle.wisc.edu/mstat/index.html). Sample sizes were chosen based on previously published work. Outliers were determined using Grubbs' Method, and excluded from analysis. Two outliers were removed from the data in Table 3 (one measurement of Cal51+10 nM, and one measurement of MDA-MB-231+10 μM paclitaxel were removed). Fixed data analysis was blinded by concealment of slide labels. p values are listed in Table S2.

Supplementary Material

Refer to Web version on PubMed Central for supplementary material.

Acknowledgments

We thank Duane Compton for NuMA antibody and Jill Kolesar and Marcy Pomplun in the UWCCC 3P core facility for performing paclitaxel measurements. We thank our patients for participating in this research.

Funding: This work was supported in part by grants from the National Institutes of Health (R01CA140458 to BAW and P30 CA014520 to UWCCC). Additional support was provided from R01CA073808 (RTR), NCATS 9U54TR000021 (AJT), T32 GM008688 (LMZ and KAA) and T32 CA009135 (LMZ).

References and Notes

1. Walsh V, Goodman J. From taxol to Taxol: the changing identities and ownership of an anti-cancer drug. Med Anthropol. 2002; 21:307–336. [PubMed: 12458837]
2. Huang TC, Campbell TC. Comparison of weekly versus every 3 weeks paclitaxel in the treatment of advanced solid tumors: a meta-analysis. Cancer Treat Rev. 2012; 38:613–617. [PubMed: 22155063]
3. Schiff PB, Fant J, Horwitz SB. Promotion of microtubule assembly in vitro by taxol. Nature. 1979; 277:665–667. [PubMed: 423966]
4. Jordan MA, Toso RJ, Thrower D, Wilson L. Mechanism of mitotic block and inhibition of cell proliferation by taxol at low concentrations. Proc Natl Acad Sci U S A. 1993; 90:9552–9556. [PubMed: 8105478]
5. Schiff PB, Horwitz SB. Taxol stabilizes microtubules in mouse fibroblast cells. Proc Natl Acad Sci U S A. 1980; 77:1561–1565. [PubMed: 6103535]
6. Waters JC, Chen RH, Murray AW, Gorbsky GJ, Salmon ED, Nicklas RB. Mad2 binding by phosphorylated kinetochores links error detection and checkpoint action in mitosis. Curr Biol. 1999; 9:649–652. [PubMed: 10375530]
7. Kops GJ, Weaver BA, Cleveland DW. On the road to cancer: aneuploidy and the mitotic checkpoint. Nat Rev Cancer. 2005; 5:773–785. [PubMed: 16195750]
8. Lara-Gonzalez P, Westhorpe FG, Taylor SS. The spindle assembly checkpoint. Curr Biol. 2012; 22:R966–980. [PubMed: 23174302]
9. Derry WB, Wilson L, Jordan MA. Substoichiometric binding of taxol suppresses microtubule dynamics. Biochemistry. 1995; 34:2203–2211. [PubMed: 7857932]
10. Waters JC, Chen RH, Murray AW, Salmon ED. Localization of Mad2 to kinetochores depends on microtubule attachment, not tension. J Cell Biol. 1998; 141:1181–1191. [PubMed: 9606210]
11. Jordan MA, Wendell K, Gardiner S, Derry WB, Copp H, Wilson L. Mitotic block induced in HeLa cells by low concentrations of paclitaxel (Taxol) results in abnormal mitotic exit and apoptotic cell death. Cancer Res. 1996; 56:816–825. [PubMed: 8631019]
12. Weaver BA, Cleveland DW. Decoding the links between mitosis, cancer, and chemotherapy: The mitotic checkpoint, adaptation, and cell death. Cancer Cell. 2005; 8:7–12. [PubMed: 16023594]
13. Rieder CL, Maiato H. Stuck in division or passing through: what happens when cells cannot satisfy the spindle assembly checkpoint. Dev Cell. 2004; 7:637–651. [PubMed: 15525526]

14. Yamada HY, Gorbsky GJ. Spindle checkpoint function and cellular sensitivity to antimitotic drugs. Mol Cancer Ther. 2006; 5:2963–2969. [PubMed: 17172401]
15. Gascoigne KE, Taylor SS. Cancer cells display profound intra- and interline variation following prolonged exposure to antimitotic drugs. Cancer Cell. 2008; 14:111–122. [PubMed: 18656424]
16. Gianni L, Kearns CM, Giani A, Capri G, Viganó L, Lacatelli A, Bonadonna G, Egorin MJ. Nonlinear pharmacokinetics and metabolism of paclitaxel and its pharmacokinetic/pharmacodynamic relationships in humans. J Clin Oncol. 1995; 13:180–190. [PubMed: 7799018]
17. Huizing MT, Keung AC, Rosing H, van der Kuij V, Wten Bokkel Huinink W, Mandjes IM, Dubbelman AC, Pinedo HM, Beijnen JH. Pharmacokinetics of paclitaxel and metabolites in a randomized comparative study in platinum-pretreated ovarian cancer patients. J Clin Oncol. 1993; 11:2127–2135. [PubMed: 7901342]
18. Wiernik PH, Schwartz EL, Strauman JJ, Dutcher JP, Lipton RB, Paietta E. Phase I clinical and pharmacokinetic study of taxol. Cancer Res. 1987; 47:2486–2493. [PubMed: 2882837]
19. Yvon AM, Wadsworth P, Jordan MA. Taxol suppresses dynamics of individual microtubules in living human tumor cells. Mol Biol Cell. 1999; 10:947–959. [PubMed: 10198049]
20. Snyder JA, Mullins JM. Analysis of spindle microtubule organization in untreated and taxol-treated PtK1 cells. Cell Biol Int. 1993; 17:1075–1084. [PubMed: 7906984]
21. Yang Z, Kenny AE, Brito DA, Rieder CL. Cells satisfy the mitotic checkpoint in Taxol, and do so faster in concentrations that stabilize syntelic attachments. J Cell Biol. 2009; 186:675–684. [PubMed: 19720871]
22. Brito DA, Yang Z, Rieder CL. Microtubules do not promote mitotic slippage when the spindle assembly checkpoint cannot be satisfied. J Cell Biol. 2008; 182:623–629. [PubMed: 18710927]
23. Eisenhauer EA, Therasse P, Bogaerts J, Schwartz LH, Sargent D, Ford R, Dancey J, Arbuck S, Gwyther S, Mooney M, Rubinstein L, Shankar L, Dodd L, Kaplan R, Lacombe D, Verweij J. New response evaluation criteria in solid tumours: revised RECIST guideline (version 1.1). Eur J Cancer. 2009; 45:228–247. [PubMed: 19097774]
24. Milas L, Hunter NR, Kurdoglu B, Mason KA, Meyn RE, Stephens LC, Peters LJ. Kinetics of mitotic arrest and apoptosis in murine mammary and ovarian tumors treated with taxol. Cancer Chemother Pharmacol. 1995; 35:297–303. [PubMed: 7828272]
25. Ryan SD, Britigan EM, Zasadil LM, Witte K, Audhya A, Roopra A, Weaver BA. Up-regulation of the mitotic checkpoint component Mad1 causes chromosomal instability and resistance to microtubule poisons. Proc Natl Acad Sci U S A. 2012; 109:E2205–2214. [PubMed: 22778409]
26. Kops GJ, Foltz DR, Cleveland DW. Lethality to human cancer cells through massive chromosome loss by inhibition of the mitotic checkpoint. Proc Natl Acad Sci U S A. 2004; 101:8699–8704. [PubMed: 15159543]
27. Michel L, Diaz-Rodriguez E, Narayan G, Hernando E, Murty VV, Benezra R. Complete loss of the tumor suppressor MAD2 causes premature cyclin B degradation and mitotic failure in human somatic cells. Proc Natl Acad Sci U S A. 2004; 101:4459–4464. [PubMed: 15070740]
28. Janssen A, Kops GJ, Medema RH. Elevating the frequency of chromosome mis-segregation as a strategy to kill tumor cells. Proc Natl Acad Sci U S A. 2009; 106:19108–19113. [PubMed: 19855003]
29. Komlodi-Pasztor E, Sackett D, Wilkerson J, Fojo T. Mitosis is not a key target of microtubule agents in patient tumors. Nat Rev Clin Oncol. 2011; 8:244–250. [PubMed: 21283127]
30. Cole NB, Sciaky N, Marotta A, Song J, Lippincott-Schwartz J. Golgi dispersal during microtubule disruption: regeneration of Golgi stacks at peripheral endoplasmic reticulum exit sites. Mol Biol Cell. 1996; 7:631–650. [PubMed: 8730104]
31. Ganem NJ, Godinho SA, Pellman D. A mechanism linking extra centrosomes to chromosomal instability. Nature. 2009; 460:278–282. [PubMed: 19506557]
32. Pihan GA, Wallace J, Zhou Y, Doxsey SJ. Centrosome abnormalities and chromosome instability occur together in pre-invasive carcinomas. Cancer Res. 2003; 63:1398–1404. [PubMed: 12649205]
33. Pihan GA, Purohit A, Wallace J, Knecht H, Woda B, Quesenberry P, Doxsey SJ. Centrosome defects and genetic instability in malignant tumors. Cancer Res. 1998; 58:3974–3985. [PubMed: 9731511]

34. Fine RL, Chen J, Balmaceda C, Bruce JN, Huang M, Desai M, Sisti MB, McKhann GM, Goodman RR, Bertino JS, Nafziger AN, Fetell MR. Randomized study of paclitaxel and tamoxifen deposition into human brain tumors: implications for the treatment of metastatic brain tumors. Clin Cancer Res. 2006; 12:5770–5776. [PubMed: 17020983]
35. Mori T, Kinoshita Y, Watanabe A, Yamaguchi T, Hosokawa K, Honjo H. Retention of paclitaxel in cancer cells for 1 week in vivo and in vitro. Cancer Chemother Pharmacol. 2006; 58:665–672. [PubMed: 16534615]
36. Komlodi-Pasztor E, Sackett DL, Fojo AT. Inhibitors targeting mitosis: tales of how great drugs against a promising target were brought down by a flawed rationale. Clin Cancer Res. 2012; 18:51–63. [PubMed: 22215906]
37. Searle J, Collins DJ, Harmon B, Kerr JF. The spontaneous occurrence of apoptosis in squamous carcinomas of the uterine cervix. Pathology. 1973; 5:163–169. [PubMed: 4718080]
38. Kerr JF, Searle J. A suggested explanation for the paradoxically slow growth rate of basal-cell carcinomas that contain numerous mitotic figures. J Pathol. 1972; 107:41–44. [PubMed: 5069401]
39. Kerr JF, Wyllie AH, Currie AR. Apoptosis: a basic biological phenomenon with wide-ranging implications in tissue kinetics. Br J Cancer. 1972; 26:239–257. [PubMed: 4561027]
40. Lowe SW, Lin AW. Apoptosis in cancer. Carcinogenesis. 2000; 21:485–495. [PubMed: 10688869]
41. Weaver BA, Silk AD, Montagna C, Verdier-Pinard P, Cleveland DW. Aneuploidy acts both oncogenically and as a tumor suppressor. Cancer Cell. 2007; 11:25–36. [PubMed: 17189716]
42. Babu JR, Jeganathan KB, Baker DJ, Wu X, Kang-Decker N, van Deursen JM. Rae1 is an essential mitotic checkpoint regulator that cooperates with Bub3 to prevent chromosome missegregation. J Cell Biol. 2003; 160:341–353. [PubMed: 12551952]
43. Ricke RM, Jeganathan KB, Malureanu L, Harrison AM, van Deursen JM. Bub1 kinase activity drives error correction and mitotic checkpoint control but not tumor suppression. J Cell Biol. 2012; 199:931–949. [PubMed: 23209306]
44. Sotillo R, Hernando E, Diaz-Rodriguez E, Teruya-Feldstein J, Cordon-Cardo C, Lowe SW, Benezra R. Mad2 overexpression promotes aneuploidy and tumorigenesis in mice. Cancer Cell. 2007; 11:9–23. [PubMed: 17189715]
45. Milross CG, Mason KA, Hunter NR, Chung WK, Peters LJ, Milas L. Relationship of mitotic arrest and apoptosis to antitumor effect of paclitaxel. J Natl Cancer Inst. 1996; 88:1308–1314. [PubMed: 8797771]
46. Symmans WF, Volm MD, Shapiro RL, Perkins AB, Kim AY, Demaria S, Yee HT, McMullen H, Oratz R, Klein P, Formenti SC, Muggia F. Paclitaxel-induced apoptosis and mitotic arrest assessed by serial fine-needle aspiration: implications for early prediction of breast cancer response to neoadjuvant treatment. Clin Cancer Res. 2000; 6:4610–4617. [PubMed: 11156210]
47. Chakravarthy AB, Kelley MC, McLaren B, Truica CI, Billheimer D, Mayer IA, Grau AM, Johnson DH, Simpson JF, Beauchamp RD, Jones C, Pietenpol JA. Neoadjuvant concurrent paclitaxel and radiation in stage II/III breast cancer. Clin Cancer Res. 2006; 12:1570–1576. [PubMed: 16533783]
48. Schmidt M, Bastians H. Mitotic drug targets and the development of novel anti-mitotic anticancer drugs. Drug Resist Updat. 2007; 10:162–181. [PubMed: 17669681]
49. Wissing MD, Carducci MA, Gelderblom H, van Diest PJ. Tales of how great drugs were brought down by a flawed rationale--letter. Clin Cancer Res. 2013; 19:1303. [PubMed: 23393074]
50. Tunquist BJ, Wood KW, Walker DH. Tales of how great drugs were brought down by a flawed rationale--letter. Clin Cancer Res. 2013; 19:1302. [PubMed: 23393075]
51. Lera RF, Burkard ME. High mitotic activity of Polo-like kinase 1 is required for chromosome segregation and genomic integrity in human epithelial cells. J Biol Chem. 2012; 287:42812–42825. [PubMed: 23105120]
52. Orth JD, Kohler RH, Foijer F, Sorger PK, Weissleder R, Mitchison TJ. Analysis of mitosis and antimitotic drug responses in tumors by in vivo microscopy and single-cell pharmacodynamics. Cancer Res. 2011; 71:4608–4616. [PubMed: 21712408]
53. Janssen A, Beerling E, Medema R, van Rheenen J. Intravital FRET imaging of tumor cell viability and mitosis during chemotherapy. PLoS One. 2013; 8:e64029. [PubMed: 23691140]
54. Jackson JR, Patrick DR, Dar MM, Huang PS. Targeted anti-mitotic therapies: can we improve on tubulin agents? Nat Rev Cancer. 2007; 7:107–117. [PubMed: 17251917]

55. Compton DA, Yen TJ, Cleveland DW. Identification of novel centromere/kinetochore-associated proteins using monoclonal antibodies generated against human mitotic chromosome scaffolds. J Cell Biol. 1991; 112:1083–1097. [PubMed: 1999466]

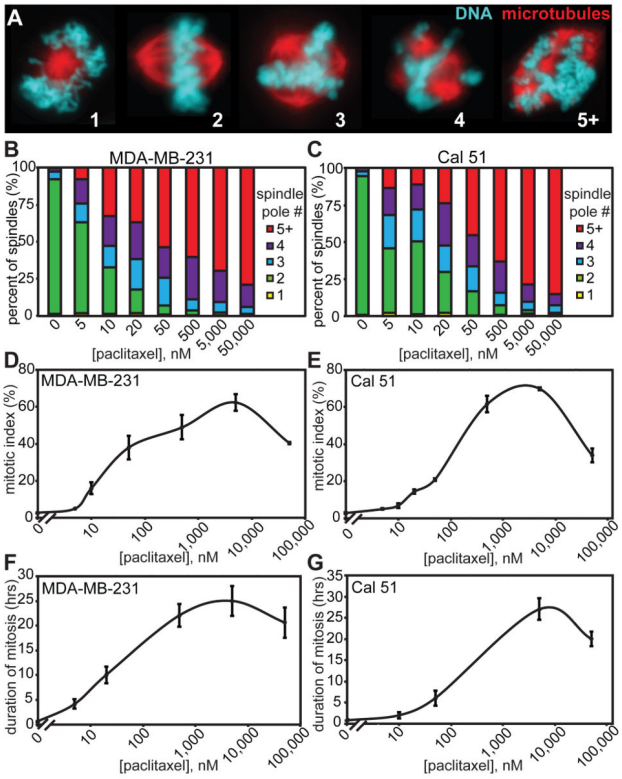

Figure 1. Paclitaxel has concentration-dependent effects

(A) Paclitaxel-treated cells exhibit mitotic spindles containing the indicated number of spindle poles as assessed by staining for microtubules (red) and DNA (teal) in MDA-MB-231 cells. (B and C) MDA-MB-231 (B) and Cal51 (C) triple negative breast cancer cell lines both show a direct relationship between number of poles per spindle and paclitaxel concentration. n ≥ 100 cells from each of 3 independent experiments. (D and E) In response to increasing concentrations of paclitaxel, mitotic index in both MDA-MB-231 (D) and Cal51 (E) cells peaks and then declines. n ≥ 1500 cells from 3 separate experiments. (F and G) Duration of mitosis in response to paclitaxel in both MDA-MB-231 (F) and Cal51 (G) cells closely mimics mitotic index. Duration of mitosis was measured as length of time from rounding to flattening of the first daughter cell in 10× phase contrast movies acquired every 10 minutes for 65 hours. n ≥ 30 cells per condition.

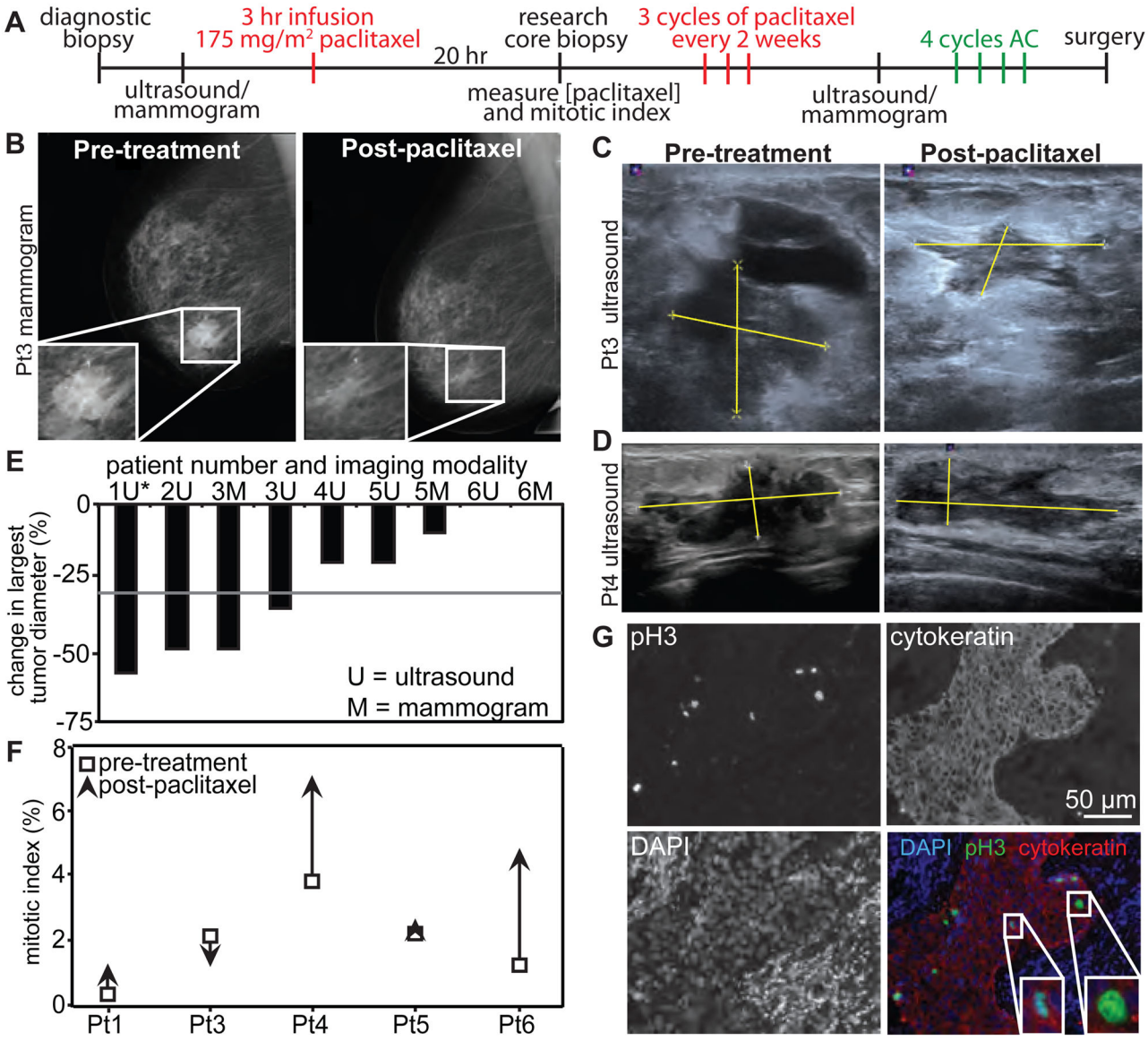

Figure 2. Mitotic arrest is not required for response to paclitaxel

(A) Schematic showing the trial design. Research biopsy and serum were obtained 20 hours after the start of the first 3 hour paclitaxel infusion. Tumor measurements were obtained by mammogram and/or ultrasound, depending on patient insurance. AC = a combination of Adriamycin and cyclophosphamide. (B through D) Mammograms (B) and ultrasounds (C, D) used to measure tumor response. Yellow lines in C and D indicate tumor measurements. (E) Waterfall plot showing change in largest tumor diameter. Response to paclitaxel is determined as a decrease of ≥30% in largest tumor diameter, according to RECIST 1.1 criteria (23). The grey line indicates this threshold. *Note that the second tumor measurement was obtained after cycle 1 of AC in patient 1, but before AC in all other patients. (F) Mitotic index before (open square) and after 20 hours of paclitaxel treatment (arrowhead; the direction indicates increase or decrease in mitotic index in response to

paclitaxel). n ≥ 500 cells. (G) Patient 5 tumor stained with phosphorylated histone H3 (pH3; to mark mitotic cells), DAPI, and cytokeratin (to identify epithelial cells). Insets, enlargements of mitotic cells. Scale bar = 50 μm.

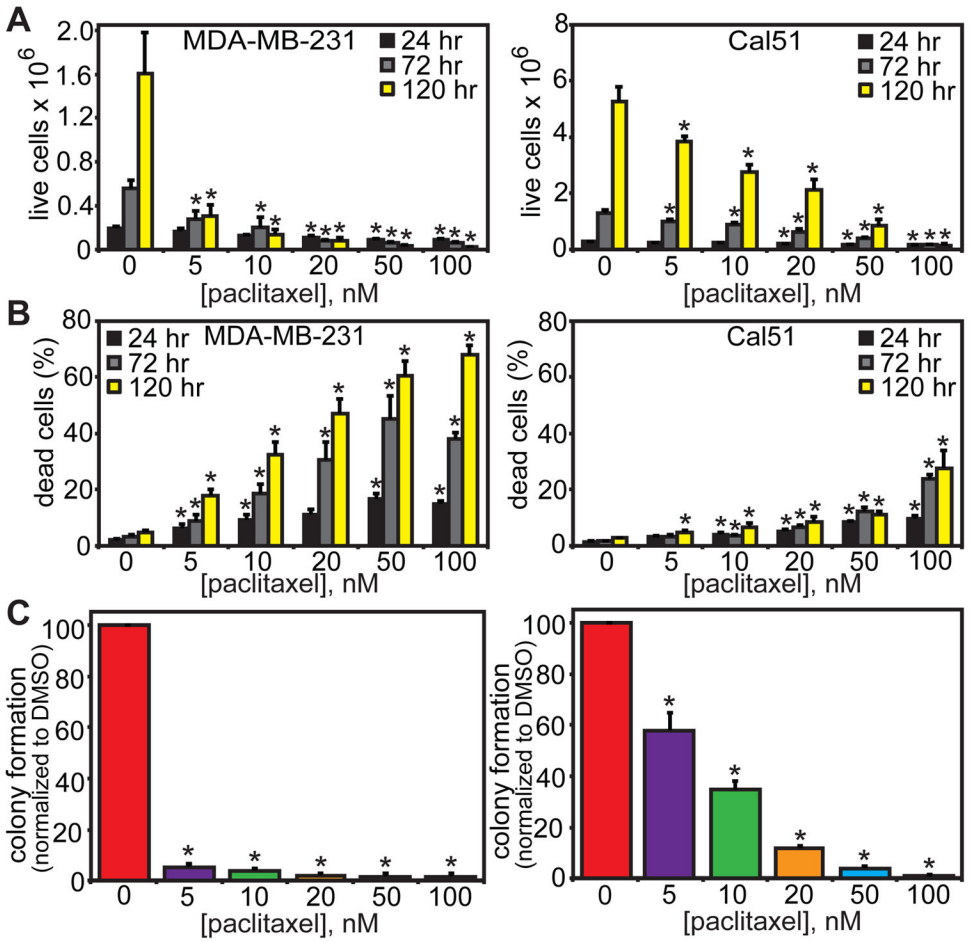

Figure 3. Clinically relevant concentrations of paclitaxel cause cell death

(A) Low nM concentrations of paclitaxel cause a decrease in live cell number over 120 hours in MDA-MB-231 (left) and Cal51 (right) cells. (B) Trypan blue assay showing an increase in the proportion of dead cells in both MDA-MB-231 (left) and Cal51 (right) cell lines by 120 hours of paclitaxel treatment. (C) Low nM paclitaxel inhibits the ability of cells to form colonies after 14 days of paclitaxel treatment. No colony formation was observed at concentrations above 100 nM paclitaxel in either cell line. (A–C) $n \geq 3$ independent experiments. * = $p < 0.05$ as compared to DMSO control by Wilcoxon (A, C) or Mantel-Haenszel (B) statistical analysis. Exact p values are listed in Table S2.

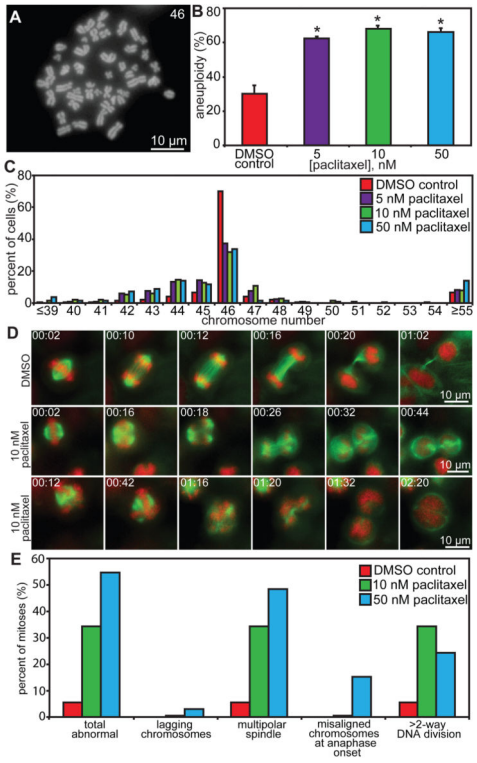

Figure 4. Low concentrations of paclitaxel increase aneuploidy and chromosome missegregation

(A) Chromosome spread from a Cal51 cell containing 46 chromosomes. (B–C) Cal51 cells treated for 48 hours with 5, 10, or 50 nM paclitaxel show an increase in aneuploidy (B) that is predominantly near-diploid with little effect on triploidy or tetraploidy (C). n = 50 cells from each of 3 independent experiments. (D–E) Low dose paclitaxel increases abnormal mitotic events. (D) Cal51 cells expressing H2B-RFP (red) and GFP-tubulin (green) were filmed at 60× with 2-minute intervals during mitosis in DMSO (top row) or 10 nM paclitaxel (center and bottom rows). Shown are still frames from Videos S1–3. Time is shown in hours:minutes. Cells are able to divide in the presence of drug on multipolar spindles. (E) Quantitation of mitotic defects in Cal51 cells. The increase in defects is mainly due to multipolar spindles and >2–way DNA divisions. n=20–36 cells per condition. * = $p < 0.05$ as compared to DMSO control by Wilcoxon statistical analysis. Exact p values are listed in Table S2.

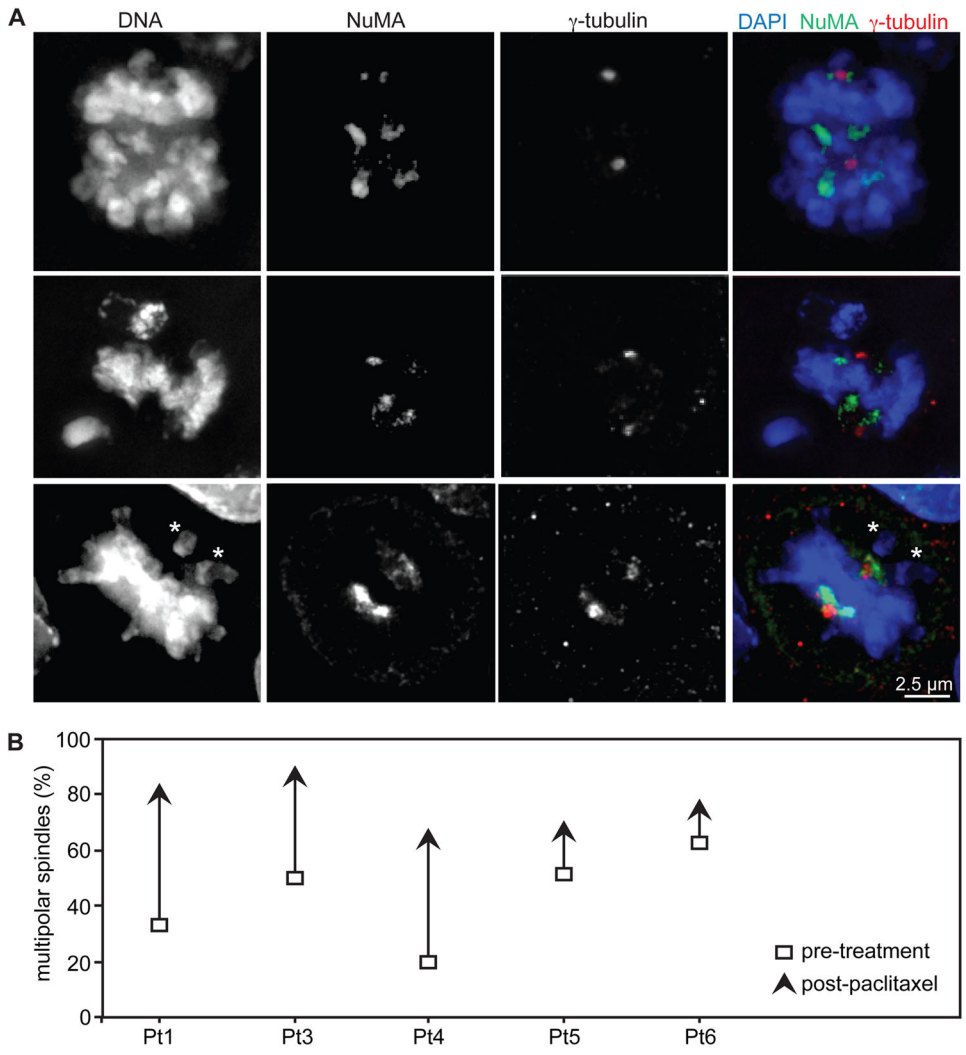

Figure 5. Paclitaxel causes multipolar spindles in patient tumors

(A) Immunofluorescence of patient tumors reveals additional spindle poles, indicated by NuMA staining. Not all poles contain γ-tubulin. Asterisks denote misaligned chromosomes, which occur even on bipolar spindles. Scale bar = 2.5 μm. (B) The incidence of multipolar spindles, defined as containing >2 NuMA foci, increased in every patient after paclitaxel treatment. Samples sizes for patients 1, 3, 4, 5 and 6, respectively, are 9, 9, 25, 53, and 19 mitotic cells pre-treatment and 11, 31, 29, 35 and 26 mitotic cells post-paclitaxel.

Sci Transl Med. Author manuscript; available in PMC 2014 September 26.

Table 1

Patient characteristics

patient #	age, years	Estrogen Receptor status	Progesterone Receptor status	# positive lymph nodes/# sampled**	Nottingham grade
1	42	positive	positive	0/17	3
2	53	negative	negative	14/14	2
3	65	negative	negative	1/22	3
4	45	negative	negative	1/11	3
5	57	positive	negative	0/20	3
6	49	positive	positive	22/23	2

Note that all patients were Caucasian, not Hispanic or Latino, and were diagnosed with HER2 negative invasive ductal carcinoma.

** at surgery

Table 2

Paclitaxel measurements in patients by tumor weight

patient #	plasma [paclitaxel], μM	tumor [paclitaxel], μM	degree of concentration
1	0.08	2.6	32×
2*	-	-	-
3	0.14	9.0	64×
4	0.11	7.7	70×
5	0.28	1.1	4×
6	0.15	2.5	17×

* skin biopsy of superficial tumor that yielded minimal tumor tissue

- = not tested.

Table 3

Paclitaxel concentration in breast cancer cells

[paclitaxel] in media, μM	MDA-MB-231				Cal51			
	non-fluorescent		GFP-tub RFP-H2B		non-fluorescent		GFP-tub RFP-H2B	
	[paclitaxel], μM (n) +/− S.E.	fold uptake	[paclitaxel], μM (n) +/− S.E.	fold uptake	[paclitaxel], μM (n) +/− S.E.	fold uptake	[paclitaxel], μM (n) +/− S.E.	fold uptake
DMSO	ND		ND		ND		ND	
0.005	3.8 (4) +/− 0.68	760×	-		0.35 (4) +/− 0.07	70×	-	-
0.01	7.0 (4) +/− 0.93	700×	16 (3) +/− 3.8	1600×	0.77 (4) +/− 0.01	77×	1.7 (3) +/− 0.15	170×
0.02	24 (3) +/− 6.0	1200×	-	-	1.5 (4) +/− 0.08	75×	-	-
0.05	33 (5) +/− 3.6	660×	-	-	3.2 (5) +/− 0.74	64×	3.3 (3) +/− 1.7	66×
0.1	29 (3) +/− 6.1	290×	89 (2) +/− 10	890×	4.6 (4) +/− 1.5	46×	9.7 (3) +/− 1.1	97×
1	75 (3) +/− 12	75×	140 (2) +/− 9.6	140×	11 (4) +/− 2.2	11×	21 (3) +/− 0.70	21×
10	420 (2) +/− 11	42×	-	-	80 (4) +/− 13	8×	-	

ND = not detected.

- = not tested.